JOURNAL OF THE AMERICAN COLLEGE OF CARDIOLOGY VOL. 74, NO. 14, 2019

KLF15-Wnt–Dependent Cardiac Reprogramming Up-Regulates SHISA3 in the Mammalian Heart

Claudia Noack, PhD,[a,b,c,*] Lavanya M. Iyer, PhD,[a,b,d,*] Norman Y. Liaw, PhD,[a,b] Eric Schoger, MS,[a,b] Sara Khadjeh, PhD,[b,e] Eva Wagner, PhD,[b,e] Monique Woelfer, PhD,[a,b] Maria-Patapia Zafiriou, PhD,[a,b] Hendrik Milting, MD,[f] Samuel Sossalla, MD,[b,e,g] Katrin Streckfuss-Boemeke, PhD,[b,e] Gerd Hasenfuß, MD,[b,e] Wolfram-Hubertus Zimmermann, MD,[a,b] Laura C. Zelarayán, PhD[a,b]

ABSTRACT

BACKGROUND The combination of cardiomyocyte (CM) and vascular cell (VC) fetal reprogramming upon stress culminates in end-stage heart failure (HF) by mechanisms that are not fully understood. Previous studies suggest KLF15 as a key regulator of CM hypertrophy.

OBJECTIVES This study aimed to characterize the impact of KLF15-dependent cardiac transcriptional networks leading to HF progression, amenable to therapeutic intervention in the adult heart.

METHODS Transcriptomic bioinformatics, phenotyping of *Klf15* knockout mice, Wnt-signaling-modulated hearts, and pressure overload and myocardial ischemia models were applied. Human *KLF15* knockout embryonic stem cells, engineered human myocardium, and human samples were used to validate the relevance of the identified mechanisms.

RESULTS The authors identified a sequential, postnatal transcriptional repression mediated by KLF15 of pathways implicated in pathological tissue remodeling, including distinct Wnt-pathways that control CM fetal reprogramming and VC remodeling. The authors further uncovered a vascular program induced by a cellular crosstalk initiated by CM, characterized by a reduction of KLF15 and a concomitant activation of Wnt-dependent transcriptional signaling. Within this program, a so-far uncharacterized cardiac player, SHISA3, primarily expressed in VCs in fetal hearts and pathological remodeling was identified. Importantly, the KLF15 and Wnt codependent SHISA3 regulation was demonstrated to be conserved in mouse and human models.

CONCLUSIONS The authors unraveled a network interplay defined by KLF15–Wnt dynamics controlling CM and VC homeostasis in the postnatal heart and demonstrated its potential as a cardiac-specific therapeutic target in HF. Within this network, they identified SHISA3 as a novel, evolutionarily conserved VC marker involved in pathological remodeling in HF. (J Am Coll Cardiol 2019;74:1804–19) © 2019 The Authors. Published by Elsevier on behalf of the American College of Cardiology Foundation. This is an open access article under the CC BY-NC-ND license (http://creativecommons.org/licenses/by-nc-nd/4.0/).

From the [a]Institute of Pharmacology and Toxicology, University Medical Center Goettingen, Georg-August University, Goettingen, Germany; [b]DZHK (German Center for Cardiovascular Research), partner site Goettingen, Germany; [c]Research & Development, Pharmaceuticals, Bayer AG, Berlin, Germany; [d]Computational and Systems Biology, Genome Institute of Singapore (GIS), Singapore; [e]Department of Cardiology and Pneumology, University Medical Center Goettingen, Georg-August University, Goettingen, Germany; [f]Erich and Hanna Klessmann Institute, Heart and Diabetes Centre NRW, University Hospital of the Ruhr-University Bochum, Bad Oeynhausen, Germany; and the [g]Department of Internal Medicine II, University Medical Center Regensburg, Regensburg, Germany. *Drs. Noack and Iyer contributed equally to this work. This work was supported by a Deutsche Forschungsgemeinschaft (DFG) grant (ZE900-3 to Dr. Zelarayán), the Collaborative Research Center (CRC/SFB) 1002 (Project C07 to Dr. Zelarayán; D01 to Dr. Hasenfuß and C04/S01 to Dr. Zimmermann), German Heart Research Foundation (F/29/7 to Dr. Zelarayán), and the German Center for Cardiovascular Research (DZHK). Dr. Noack is an employee of Bayer. Dr. Hasenfuß has received speakers fees from AstraZeneca, Berlin Chemie, Corvia, Impulse Dynamics, Novartis, Servier, and Vifor Pharma; has been a consultant for Corvia, Impulse Dynamics, Novartis, Servier, and Vifor Pharma; and is co-principal investigator for Impulse Dynamics. Dr. Zimmermann is a co-founder and shareholder of myriamed GmbH and Repairon GmbH. All other authors have reported that they have no relationships relevant to the contents of this paper to disclose.

Manuscript received September 18, 2018; revised manuscript received May 31, 2019, accepted July 12, 2019.

Listen to this manuscript's audio summary by Editor-in-Chief Dr. Valentin Fuster on JACC.org.

ISSN 0735-1097 https://doi.org/10.1016/j.jacc.2019.07.076

Hypertrophy and heart failure (HF) are characterized by cardiomyocytes (CMs) and interstitial cells undergoing a phenotypic change, including altered cell-cell interactions (1) resulting in fibrosis, and loss of contractile muscle and capillary density. Capillary density decreases during the transition from cardiac hypertrophy to HF in patients (2). Thus, there is a functional association between CM hypertrophy and inefficient myocardial angiogenesis/vasculogenesis. However, the molecular and cellular players involved within this link are not fully elucidated.

Many signaling systems are known to regulate the complexity of cellular interactions in the adult heart, including Wnt/β-catenin (canonical) signaling (3). In the healthy heart, Wnt/β-catenin-dependent signaling is very low, becoming increased upon injury/stress through its activity in different cell types (3-5). We previously demonstrated that Krueppel-like factor 15 (KLF15) is necessary for repressing Wnt/β-catenin signaling in the healthy heart (6). KLF15 is mainly expressed in CM and fibroblasts, controlling gene expression (7). In CM, KLF15 represses pro-hypertrophic signaling pathways including Myocyte enhancer factor-2 (MEF2)-, GATA4-, and serum response factor (SRF)-dependent transcription (8,9). In fibroblasts, KLF15 inhibits connective tissue growth factor (CTGF) expression (10). In line with Wnt/β-catenin signaling activation, KLF15 expression is reduced in human and mouse cardiomyopathies (9,11). KLF15-mediated mechanisms coordinating transcriptional networks and how this affects cellular cross-talk in the postnatal heart have yet to be elucidated.

SEE PAGE 1820

In this study, we report a cardiac-specific role for KLF15 in the regulation of Wnt signaling and uncover its transcriptional network controlling adult heart homeostasis and disease. We further identify a novel vascular factor, *Shisa3*, which is activated in pathological remodeling in murine and human hearts. We report the impact of KLF15 and Wnt regulation in human myocardial cells.

METHODS

MOUSE MODELS. C57BL/6 *Klf15* knockout (KO) and the CM-specific β-catenin gain-of-function (β-Cat$^{\Delta ex3}$) models were previously described (4,6). Transverse aortic constriction (TAC) and myocardial infarction (MI) was performed in 12-week-old mice. Mice were sacrificed at 1, 2, 4, and 8 weeks post-interventions, and hearts were excised for examination. Echocardiography analyses were performed using a VisualSonics Vevo 2100 system (FUJIFILM VisualSonics, Toronto, Ontario, Canada). Genotyping primers as well as preanesthetic, anesthetic and pain relief agents used for interventions in mice are listed in Online Tables 1 and 2. All animal experiments were approved by the Lower Saxony Animal Review Board (LAVES, AZ-G15-1840).

RNA SEQUENCING AND DATA ANALYSES. RNA sequencing (RNA-seq) was performed at the Next-generation Sequencing Integrative Genomics Core Unit (NIG), University Medical Center Goettingen, Germany. Total RNA was extracted; quality and integrity were assessed using the Fragment Analyzer (Agilent, Santa Clara, California). TruSeq RNA Library Preparation Kit v2 was used (Cat no RS-122-2001; Illumina, San Diego, California). Sequencing was performed in triplicates using the HiSeq2500 (single read; 1 × 50 base pairs; 30 million reads/sample). Sequence images were transformed with Illumina software BaseCaller, demultiplexed to fastq files with CASAVA v1.8.2 software (Illumina) and aligned to the mouse reference assembly (UCSC version mm9) using TopHat version 2.1.0 software (Center for Computational Biology at Johns Hopkins University, Baltimore, Maryland) (12). Gene ontology analyses were performed using Cytoscape ClueGO (13). Gene set enrichment analysis performed was based on the entire RNA-seq profile and pathways retrieved from Molecular Signature database (MSigdb) (14) (NCBI GEO under accession numbers GSE97763 and GSE113027).

IMMUNOHISTOCHEMISTRY. Ventricular human tissue was obtained from explanted hearts of end-stage HF patients and nonfailing donors (could not be transplanted due to technical reasons) (Online Table 3). All procedures were performed according to the Declaration of Helsinki and were approved by the local ethics committee (AZ-31/9/00). Human and murine hearts were embedded in paraffin, sectioned, deparaffinized, rehydrated, and then antigens were unmasked. Sections were blocked and subsequently incubated with primary and secondary antibodies (Online Table 4). Microscopic images were captured with a confocal microscope (Zeiss 710; Carl Zeiss, Oberkochen, Germany).

STATISTICAL ANALYSES. Unpaired Student's *t*-test, Welch's *t*-test, 1-way analysis of variance followed by

ABBREVIATIONS AND ACRONYMS

CM = cardiomyocyte
cTnT = cardiac troponin T
CVD = cardiovascular disease
DEG = differentially expressed gene
E = embryonic day
EC = endothelial cell
EHM = engineered human myocardium
EMCN = endomucin
HES = human embryonic stem cell
HF = heart failure
KLF15 = Krueppel-like factor 15
KO = knockout
MI = myocardial ischemia
P = postnatal day
RNA-seq = RNA sequencing
SMC = smooth muscle cell
TAC = transverse aortic constriction
TF = transcription factor
VC = vascular cell
WT = wild-type

FIGURE 1 Sequential Wnt Signaling Derepression in *Klf15* KO Hearts

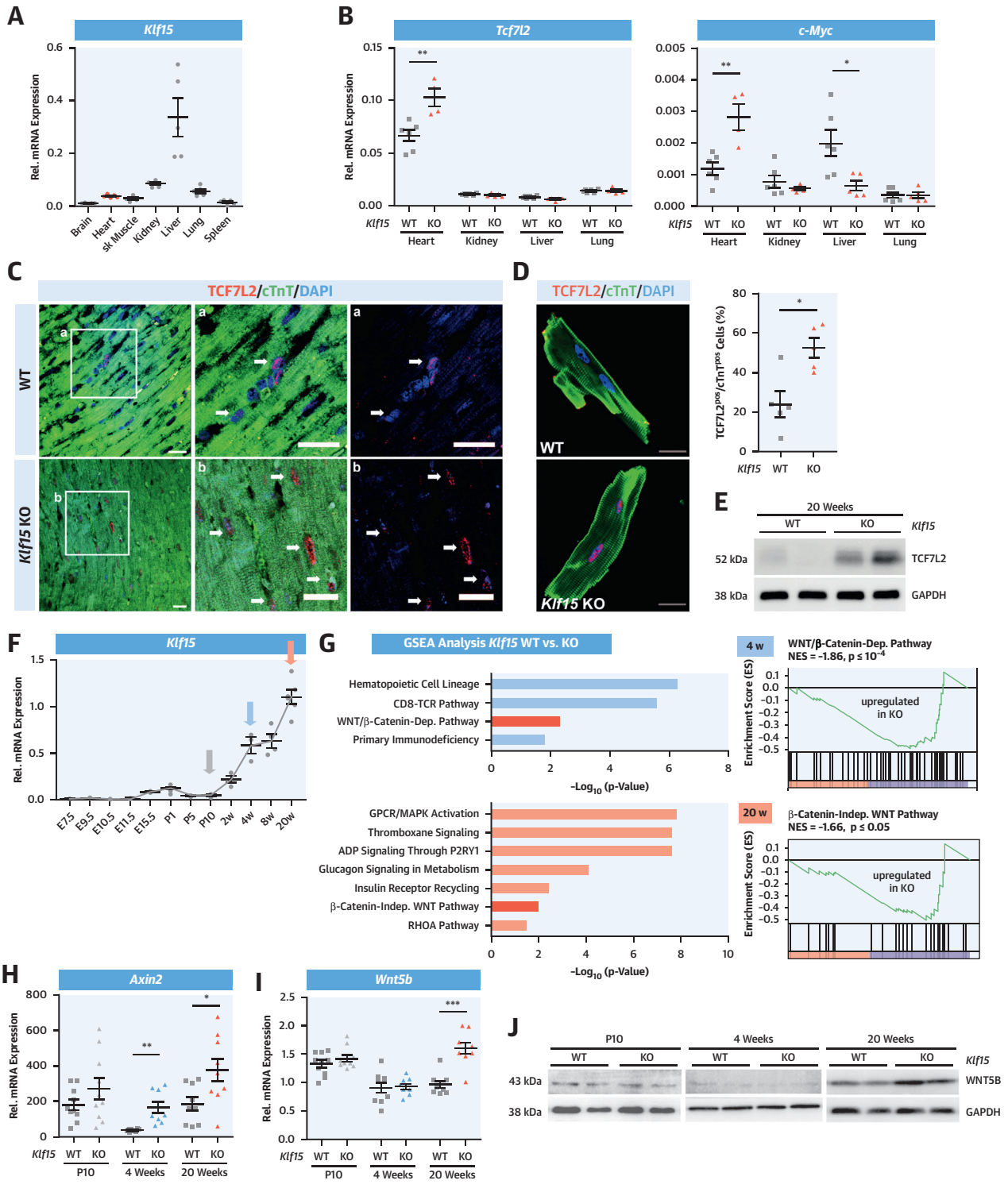

Continued on the next page

Bonferroni's multiple comparison test, or 2-way analysis of variance with Tukey's multiple comparison test (GraphPad Prism 8.0, GraphPad Software, San Diego, California) were used where appropriate for statistical analysis. Data are presented as mean ± SEM, with p values ≤0.05 considered statistically significant.

RESULTS

KLF15 IS A CARDIAC-SPECIFIC HOMEOSTATIC REGULATOR OF THE WNT/β-CATENIN–DEPENDENT AND –INDEPENDENT PATHWAYS IN THE POSTNATAL HEART. In line with the repressive function of KLF15 on Wnt/β-catenin-dependent signaling, we showed that although the highest expression of *Klf15* transcripts were found in liver, followed by kidney, lung, heart, and skeletal muscle (**Figure 1A**), the expression of *Tcf7l2*, the main cardiac transcriptional activator of the Wnt/β-catenin pathway and its ubiquitous target *c-Myc* (4,15) was increased only in heart tissues of *Klf15* KO adult mice (6) (**Figure 1B**). Greater TCF7L2 expression in cardiac troponin T (cTnT)-positive CM of *Klf15* KO mice was observed by confocal analysis in tissue and isolated CMs, and further confirmed by Western blot analysis of whole-heart lysates (**Figures 1C to 1E**, Online Figures 1A and 2A and 2B). Collectively, these findings indicate a heart-specific, KLF15-mediated repression of Wnt/β-catenin-dependent signaling. Interestingly, physiological *Klf15* mRNA expression begins to rise postnatally at 2 weeks in wild-type (WT) hearts, coinciding with the physiological decay in Wnt activity (**Figure 1F**, Online Figure 3A). In *Klf15* KO mice, functional deterioration was observed only beyond 12 weeks, supporting our previous data (Online Figure 3B, Online Table 5) (6). Hence, *Klf15* KO hearts provide an ideal starting point to unravel sequential regulatory pathways driving HF progression. On the basis of the time course of HF development in *Klf15* KO and physiological *Klf15* expression, we performed RNA-seq in the following models (**Figure 1F**): 1) postnatal day (P) 10 (resembling low physiological *Klf15* expression in WT hearts and normal heart function in *Klf15* KO) as healthy; 2) 4 weeks (resembling high physiological *Klf15* expression in WT hearts and normal heart function in *Klf15* KO) as transition to HF; and 3) 20 weeks (resembling high physiological *Klf15* expression in WT hearts; fetal gene re-expression and cardiac failure in *Klf15* KO mice) as symptomatic HF (Online Figure 3C and 3D). Principal component analysis showed that WT P10 were clearly separated from WT 4-week and WT 20-week samples, whereas WT P10 and the KOs at all ages were closely clustered in PC1 (First Principal Component) (Online Figure 3E), suggesting that *Klf15* KO maintains an immature cardiac transcriptional profile. Compared with WT hearts, *Klf15* KO resulted in 92, 183, and 219 up-regulated (derepressed) genes at P10, 4 weeks, and 20 weeks, respectively, suggesting KLF15 plays increasingly suppressive roles from early life to adulthood. By contrast, 318, 254, and 359 down-regulated genes were detected in *Klf15* KO hearts at P10, 4 weeks, and 20 weeks, respectively, indicating that KLF15 has stable, activating transcriptional functions at all analyzed postnatal stages (n = 3/stage; $p < 0.05$, $\log_2 FC \geq 0.5$, heatmaps and list of differentially expressed genes [DEGs] shown in Online Figure 3F, Online Table 6). Gene set enrichment analysis showed that the Wnt/β-catenin-dependent pathway was enriched only at 4 weeks followed by β-catenin-independent Wnt signaling and Rho-A pathways enrichment at 20 weeks in *Klf15* KO hearts, validated by increased expression of *Axin2*, *Sox4*, *Cd44* (β-catenin-dependent) and *Wnt5b* (β-catenin-independent), respectively. *Wnt5b* regulation was confirmed at the protein level. Increased *Tcf7L2* was validated in 16-week, but not in 2-week old *Klf15* KO hearts (**Figures 1G to 1J**, Online Figures 1B and 3G to 3I). These results indicate progressive Wnt/β-catenin-dependent and -independent activation followed by HF in *Klf15* KO mice.

FIGURE 1 Continued

(A) qPCR of *Klf15* and **(B)** Wnt targets *Tcf7l2* and *c-Myc* in adult murine organs of WT and *Klf15* KO mice; n ≥ 5. **(C)** Immunofluorescence showing TCF7L2 in cTnT-positive CMs in hearts **(white arrows, a and b)** and **(D)** in isolated CMs with corresponding quantification and **(E)** whole-heart TCF7L2 Western blot in 20-week WT and *Klf15* KO. **Boxed areas a and b in C (left)** are shown at higher magnification in the **middle and right panels**. **(F)** *Klf15* expression in murine cardiac embryonic, postnatal, and adult stages; n ≥ 3/stage. **Arrows** indicate the time point for RNA sequencing. **(G)** Gene set enrichment analysis (GSEA) in 4-week and 20-week *Klf15* KO hearts compared with WT. A positive value indicates correlation with the WT phenotype, a negative value with the KO phenotype. **(H)** qPCR validations of the Wnt/β-catenin–dependent target *Axin2*; **(I)** β-catenin–independent *Wnt5b* transcript and **(J)** WNT5B protein in P10, 4-week, and 20-week *Klf15* KO hearts; n ≥ 9. Scale bar in **C** and **D** = 20 μm. GAPDH was used as the loading control. qPCR was normalized in **A**, **B**, and **F** to *β-actin*, and in **H to I** to *Tbp*. *p ≤ 0.05, **p ≤ 0.01, ***p ≤ 0.001 by unpaired Student's *t*-test **(B, D, I)** and with Welch's correction **(H)**. CM = cardiomyocyte; E = embryonic day; KO = knockout; P = postnatal day; qPCR = quantitative polymerase chain reaction; w = week; WT = wild-type.

FIGURE 2 ***Klf15* KO Hearts Decrease Metabolic Processes and Activate Tissue Remodeling Processes**

(A) Gene ontology [−log10 (p value)] biological processes (GO-BP) of up- and down-differentially expressed genes (DEGs) (log2FC $> \pm 0.5$ and $p < 0.05$) in P10, 4-week, and 20-week *Klf15* KO ventricles. Venn diagram and GO-BP of **(B)** common DEGs (up in 4 and 20 weeks or down in all ages) of *Klf15* KO hearts and of **(C)** genes bound by KLF15 (chromatin immunoprecipitation sequencing), and repressed or activated (DEGs from RNA sequencing) in 4-week and 20-week *Klf15* KO mice hearts versus control WT. Wnt signaling is highlighted by the **red bar**. Abbreviations as in Figure 1.

FIGURE 3 ***Klf15* KO and Wnt-Activated Hearts Show Common Pathological Mechanisms**

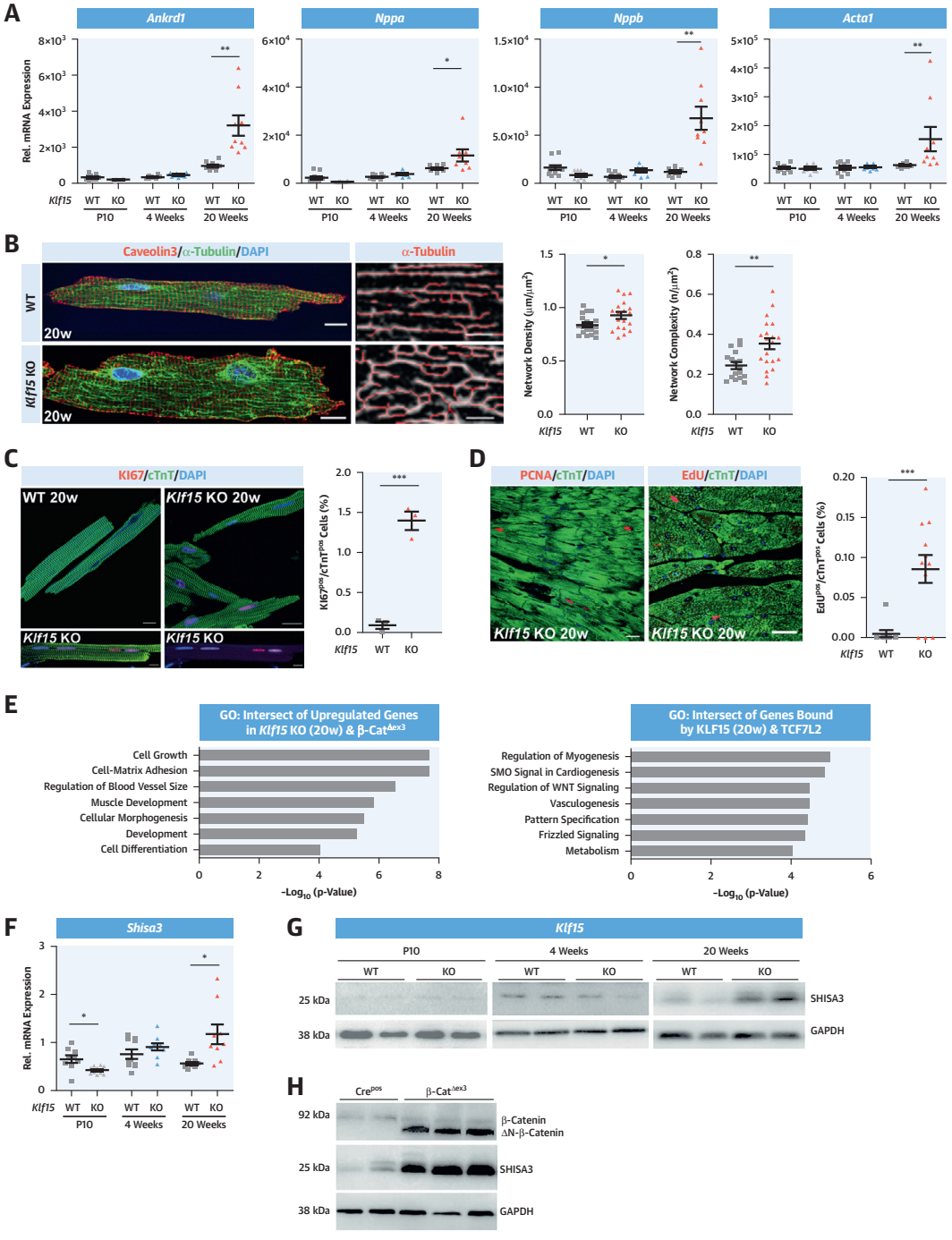

(A) Increased fetal gene transcripts only at 20 weeks in *Klf15* KO versus WT hearts. Immunofluorescence and quantification showing **(B)** CM cytoskeletal network density and complexity (Caveolin3: membrane; α-tubulin: microtubule; DAPI: nuclei; n ≥ 5 mice); cell cycling **(C)** KI67 in isolated CM and **(D)** PCNA and EdU^{+}/cTnT^{+} cells in tissue with corresponding quantification from *Klf15* KO and WT hearts; n = 3/≥10 cells/mice. **(E)** GO-BP of commonly up-regulated genes in *Klf15* KO and β-Cat$^{\Delta ex3}$ hearts, and genomic regions commonly bound by KLF15 in the healthy adult and TCF7L2 in Wnt-activated-diseased heart (β-Cat$^{\Delta ex3}$). **(F)** qPCR (n ≥ 9) and **(G)** immunoblot of SHISA3 in *Klf15* KO and **(H)** in β-Cat$^{\Delta ex3}$ hearts (showing β-catenin stabilization). Scale bar in **B** =10 μm; and in **C and D**, 20 μm. GAPDH was used as the loading control. qPCR was normalized to *Tbp*. *p ≤ 0.05, **p ≤ 0.01, ***p ≤ 0.001 by unpaired Student's *t*-test with Welch's correction. Abbreviations as in Figures 1 and 2.

FIGURE 4 **SHISA3 Is Up-Regulated in Pathological Heart Remodeling**

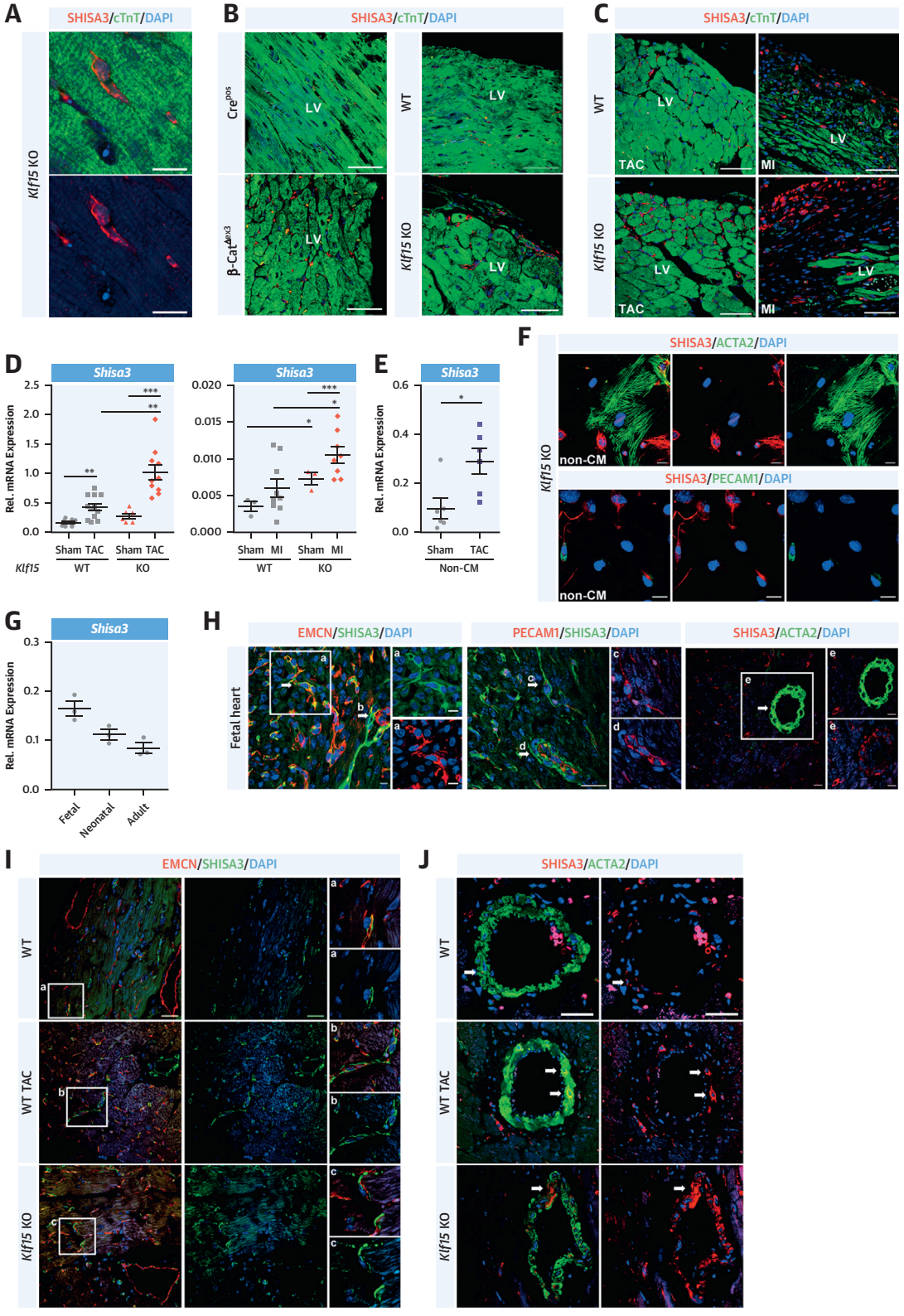

Continued on the next page

KLF15 SEQUENTIALLY REPRESSES PATHOLOGICAL REPROGRAMMING PATHWAYS. Gene ontology analysis of up-regulated DEGs in *Klf15* KO hearts showed developmental pattern formation at P10; chromatin modifications, cell cycle, muscle contraction, and endothelial development at 4 weeks; and cell growth, cardiac muscle and endothelial development at 20 weeks. Down-regulated genes in *Klf15* KO hearts included mainly amino acid, carbohydrate, and fatty acid metabolism, independent of age (**Figure 2A**). Only 7 up-regulated genes overlapped among all ages. A greater overlap was detected between 4 weeks and 20 weeks (23 genes), annotating to tissue remodeling processes and branching morphogenesis. Down-regulated genes showed more overlap between all the ages (53 genes) and mainly categorized into amino acid, carbohydrate, and fatty acid metabolism (**Figure 2B**, Online Figure 4A, Online Table 7). Accordingly, intersection of published KLF15 chromatin immunoprecipitation sequencing data in the adult heart (16) (2,363 genes) with our DEGs in 4 weeks and 20 weeks *Klf15* KO hearts showed that KLF15-bound genes down-regulated in *Klf15* KO (74 genes) categorized to metabolic genes (representative KLF15 occupancies on *Aldh9a1* and *Fads1* in Online Figure 4B). Conversely, bound up-regulated genes (48 genes) in KO were enriched in cellular remodeling processes including Wnt signaling pathways (**Figure 2C**). For example, KLF15 binds at the promoter region of the Wnt target *Axin2*, lowly expressed in the healthy heart, but activated in the diseased heart with higher TCF7L2 occupancy and H3K27ac enrichment (mark for transcriptionally active chromatin [17]) (Online Figure 4C, Online Table 8). These data provide evidence for direct KLF15 binding to proximal regulatory regions of silenced cardiac Wnt targets in the healthy heart.

COMMON TRANSCRIPTIONAL REPROGRAMMING PROCESSES IN KLF15 KO AND CM-WNT/β-catenin/TCF7L2–activated HEARTS. In line with pathological features in *Klf15* KO hearts, fetal genes (i.e., *Nppa*, *Nppb*, *Ankrd1*, *Acta1*) were up-regulated only in 20 weeks, but not in 4 weeks or P10 *Klf15* KO hearts (**Figure 3A**, Online Figure 5A). An insignificant up-regulation can be detected from 8 weeks for *Nppa*, *Nppb* (Online Figures 3C and 3D), suggesting a progressive regulation. Microtubule densification, and increased DNA synthesis and hypertrophy, which are characteristics of CM dedifferentiation and tissue remodeling (18), were confirmed in *Klf15* KO CM at 20 weeks (**Figures 3B to 3D**, Online Figures 5B to 5E). To discern KLF15-mediated remodeling processes depending on Wnt signaling, we investigated commonly up-regulated genes in *Klf15* KO and β-Cat$^{\Delta ex3}$ hearts with Wnt/TCF7L2/β-catenin activation in CM (4). This identified enrichment of cell growth, muscle development, and blood vessel morphogenesis processes. Overlapped genes bound by TCF7L2 and KLF15 in the adult heart showed enrichment in developmental processes, including Wnt signaling activation and vasculogenesis (**Figure 3E**).

Downstream of Wnt and KLF15, we observed significant up-regulation of Wnt canonical modulators including SHISA3 in hearts of both 20-week *Klf15* KO mice and a mouse model of CM-Wnt/β-catenin activation, β-Cat$^{\Delta ex3}$ (4) (**Figures 3F to 3H** and Online Figures 1B and 5F). Due to the role of SHISA3 as a developmental Wnt inhibitor, we were interested in its regulation in the context of cardiac remodeling. *Shisa3* along with Wnt activation remained activated in 52-week *Klf15* KO hearts, indicating a persistent activation (Online Figure 5G).

SHISA3, A NOVEL VASCULAR MARKER, IS UP-REGULATED IN PATHOLOGICAL HEART REMODELING. SHISA3 expression in *Klf15* KO and β-Cat$^{\Delta ex3}$ hearts was observed in interstitial, cTnT-negative, elongated cells (**Figure 4A**). In healthy control myocardium (WT and Cre^{pos} control), SHISA3 cells were few, but increased in *Klf15* KO and β-Cat$^{\Delta ex3}$ hearts and those with TAC- or MI-induced pathological heart

FIGURE 4 Continued

(A and B) Immunofluorescence of SHISA3^{+}/cTnT-negative cells in left ventricle (LV) in *Klf15* KO and CM-specific β-catenin stabilization (β-Cat$^{\Delta ex3}$) compared with controls (WT/Cre^{pos}), n = 3; and **(C)** in 2 weeks post-TAC and 4 weeks post-MI in WT and *Klf15* KO hearts. qPCR analysis of *Shisa3* expression in **(D)** 2-week post-TAC and 4-week post-MI hearts; and **(E)** in non-CM 2-week WT post-TAC; n = 6. **(F)** Partial colocalization of SHISA3 with ACTA2 and PECAM1 in enzymatically isolated non-CMs of adult *Klf15* KO, n = 5. **(G)** qPCR analysis of cardiac *Shisa3* from fetal (E15.5), neonatal (P3), and adult (20w) mice, n = 3. **(H)** Colocalization of SHISA3 with EMCN **(arrow *a*)**, PECAM1 **(arrow *c*)** in interstitial cells of fetal hearts (E18.5) and with ACTA2 in vessel-like structures **(arrow *e*)**. PECAM1 and EMCN positive cells in vessel were not colocalized with SHISA3 cells **(arrows *b* and *d*)**. **(I)** Colocalization of SHISA3 with EMCN and **(J)** ACTA2 in WT, 8-week post-TAC, and 20-week-old *Klf15* KO hearts. **Boxed areas a, b, and c (left)** in **I** are shown at higher magnification in the **right panels**. Scale bars in **A and F** = 10 μm; **B and C** = 50 μm; and **H to J** = 20 μm. qPCR in **D and E** was normalized to *Tbp*; *p ≤ 0.05, **p ≤ 0.01, ***p ≤ 0.001 by 1-way analysis of variance with Bonferroni's multiple comparison test **(D)** and unpaired Student's *t*-test **(E)**. ACTA2 = actin, alpha 2, smooth muscle; EMCN = endomucin; MI = myocardial infarction; TAC = transverse aortic constriction; other abbreviations as in **Figures 1 and 2**.

FIGURE 5 SHISA3 and Fetal Endothelial Marker in Remodeling

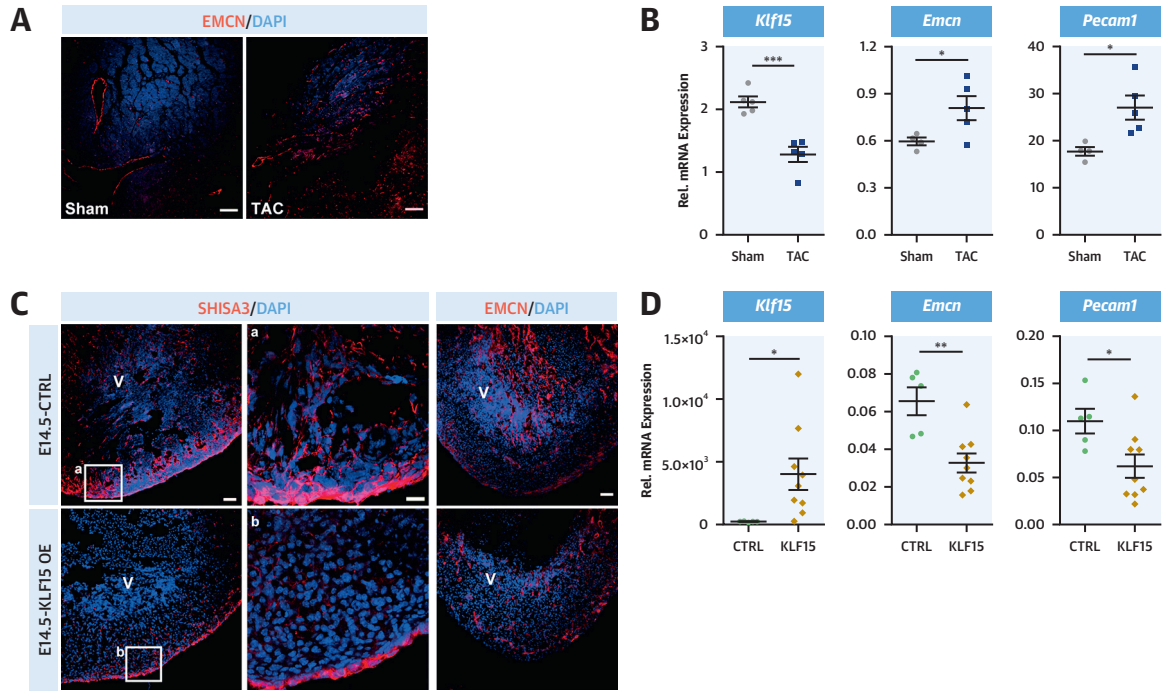

(A) EMCN expression and **(B)** qPCR validating down-regulated *Klf15* with increased *Emcn* and *Pecam1* expression in 8-week post-TAC WT hearts, n ≥ 5. **(C)** Immunofluorescence showing reduced SHISA3 and EMCN expression, and **(D)** *Emcn* and *Pecam1* down-regulation in *Klf15*-overexpressing (OE) E14.5 versus GFP control (CTRL) in fetal ventricles (V); n ≥ 5 for 2 independent experiments. **Boxed areas a and b (left)** in **C** are shown at higher magnification in the **middle panels**. qPCR was normalized to *Tbp*. Scale bars in A and C = 20 μm. *p ≤ 0.05, **p ≤ 0.01, ***p ≤ 0.001 by Student's *t*-test. Abbreviations as in Figures 1 and 4.

remodeling (validation of HF model in Online Figures 6A and 6B) (**Figures 4B and 4C**, Online Figure 6C). *Shisa3* was up-regulated during compensatory (transition) and failing phases, 1 week and 8 weeks post-TAC, respectively (Online Figures 6D and 6E). This up-regulation was exacerbated in TAC/MI *Klf15* KO hearts, in accordance with a more severe phenotype in these mice (6,9) (**Figure 4D**). *Shisa3* up-regulation was confirmed in enzymatically isolated non-CMs 2 weeks post-TAC in WT and *Klf15* KO mice (**Figure 4E**, Online Figures 6F and 6G). SHISA3 colocalized with few ACTA2^{+} and to a lesser extent with PECAM1^{+} cells in *Klf15* KO mice (**Figure 4F**).

The high fetal *Shisa3* expression decreases in postnatal heart stages (**Figure 4G**). In fetal hearts, SHISA3^{+} cells colocalized extensively with the early endothelial cell (EC) marker endomucin (EMCN) (19) and to a lesser extent with the late EC marker, PECAM1 in interstitial cells, whereas coexpression with the smooth muscle cell (SMC) marker ACTA2 was mainly found in blood vessel-like structures (**Figure 4H**). SHISA3/EMCN and SHISA3/ACTA2 colocalization was increased post-TAC and in adult *Klf15* KO hearts (**Figures 4I and 4J**). In WT ventricles, post-TAC *Shisa3* up-regulation was accompanied by reduced levels of *Klf15* and increased *Emcn* and *Pecam1* expression (**Figures 5A and 5B**). Accordingly, ex vivo overexpression of *Klf15* in fetal hearts (embryonic day [E] 14.5) (validation shown in Online Figure 7A) markedly reduced SHISA3, *Emcn* and *Pecam1* expression in comparison to GFP controls (**Figures 5C and 5D**).

Analysis of published data (20) showed increased H3K4me3 enrichment (transcriptionally active chromatin) on the *Shisa3* promoter in Flk1-positive mouse embryonic hemangioblasts upon EC differentiation (Online Figure 7B). These data indicate that SHISA3 cells belong to a fetal vascular lineage, which is reactivated upon adult heart remodeling.

A CELLULAR CROSSTALK TRIGGERS EC REPROGRAMMING UPON WNT ACTIVATION IN CM. Our present data

FIGURE 6 **Loss of *Klf15* and Wnt Activation Induce Vascular Programing**

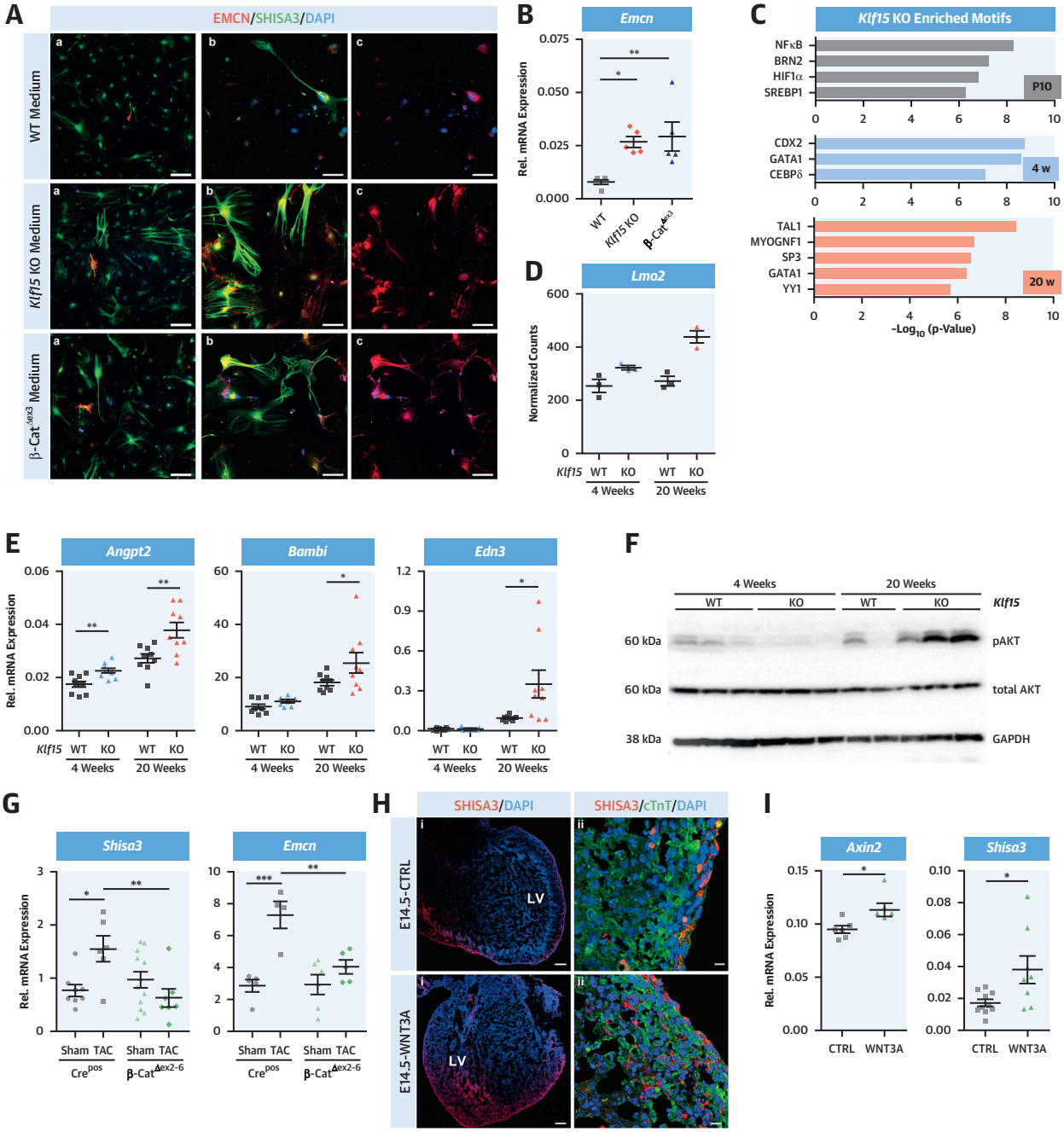

(A) SHISA3/EMCN immunofluorescence in non-CMs treated with *Klf15* KO, β-Cat$^{\Delta ex3}$-CM and WT-CM conditioned medium. **(B)** qPCR validation of *Emcn* up-regulation. **(C)** Enriched TFs in up-regulated DEGs of P10, 4-week, and 20-week *Klf15* KO hearts. **(D)** Normalized counts of the TAL1 cofactor *Lmo2* (n = 3) and **(E)** qPCR validation of *Angpt2*, *Bambi*, and *Edn3* in 4-week and 20-week *Klf15* KO hearts, n ≥ 9. **(F)** Total and pS472/pS473-AKT Western blot in 20-week *Klf15* KO hearts. **(G)** *Shisa3* and *Emcn* transcript levels in a mouse model with attenuated Wnt activation (β-Cat$^{\Delta ex2\text{-}6}$) pre- and post-TAC, n ≥ 7. **(H)** Increased SHISA3^{+}/cTnT-negative cells; **(I)** *Axin2* and *Shisa3* transcripts in E14.5 hearts treated with WNT3A conditioned medium versus control (CTRL), n = 3 to ≥8 hearts/group and experiment. Scale bar in **A-a** = 200 μm; in **A-b and A-c**, 100 μm; in **H-i**, 100 μm; and in **H-ii**, 20 μm. qPCR was normalized to *Tbp*. *p ≤ 0.05, **p ≤ 0.01, ***p ≤ 0.001 by 1-way analysis of variance with Bonferroni's multiple comparison test **(B and G)** and unpaired Student's *t*-test with Welch's correction **(E and I)**. TF = transcription factor; other abbreviations as in Figures 1 and 4.

FIGURE 7 ***KLF15* Loss Mimics Murine Function in Human Myocardium**

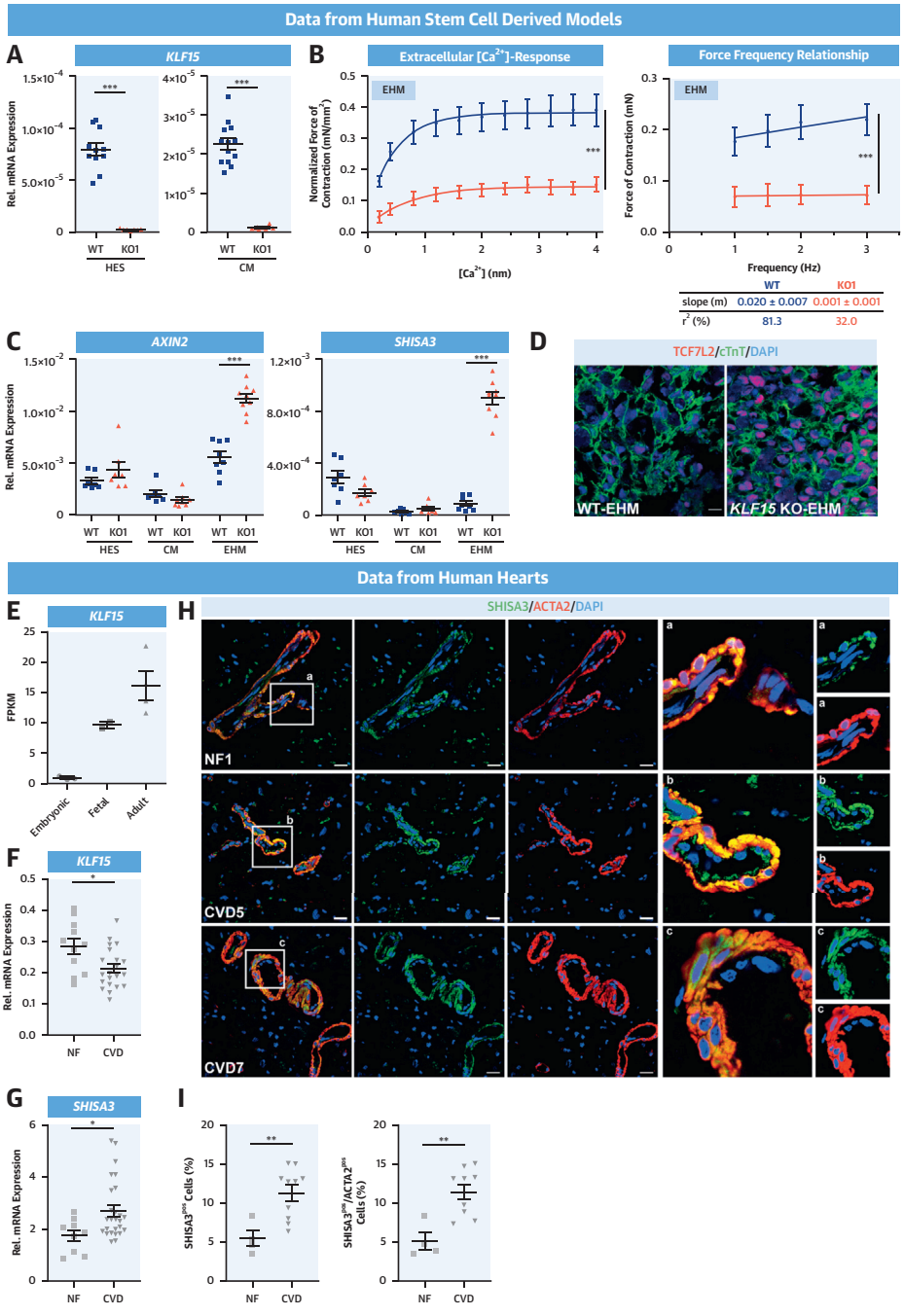

(A) qPCR validating *KLF15* loss in both human embryonic stem cells (HES) and HES-derived cardiomyocytes (CM) in *KLF15* KO compared with WT; n ≥ 7. **(B)** *KLF15* KO1 engineered human myocardium (EHM) exhibits reduced extracellular Ca^{2+} response and force–frequency relationship, n ≥ 6/group/line and experiment (total of 3, using 3 independent batches of CM differentiations). **(C)** Increased *AXIN2* and *SHISA3* expression as well as **(D)** TCF7L2 expression in cTnT CMs in *KLF15* KO EHMs but not in *KLF15* HES or *KLF15* HES-derived CMs (in 2D), n ≥ 9. **(E)** FPKMs of *KLF15* expression in human embryonic CM, and fetal and adult hearts, n = 3. **(F and G)** qPCR showing *KLF15* and *SHISA3* expression in human heart samples of nonfailing (NF) (n = 11) versus cardiovascular disease (CVD) patients (n = 35). **(H)** Representative images of SHISA3 staining in human heart sections of NF1 and dilated cardiomyopathies (CVD5/7) colocalizing with ACTA2 in vessel-like structures **(boxed areas a, b, and c)** and **(I)** corresponding semiquantification. **Boxed areas a, b, and c (left)** in **H** are shown at higher magnification in the **far right panels**. Scale bar in **D and H** = 20 μm. qPCR was normalized to *GAPDH*. *p ≤ 0.05, **p ≤ 0.01, ***p ≤ 0.001 by 2-way analysis of variance with Tukey's multiple comparison test **(B)**, unpaired Student's *t*-test **(F, G, I)**, and with Welch's correction **(A and C)**. FPKM = fragments per kilobase of exon model per million reads mapped; other abbreviations as in Figure 1.

CENTRAL ILLUSTRATION **KLF15-Wnt Signaling Controls SHISA3 and Pathological Vascular Reprogramming**

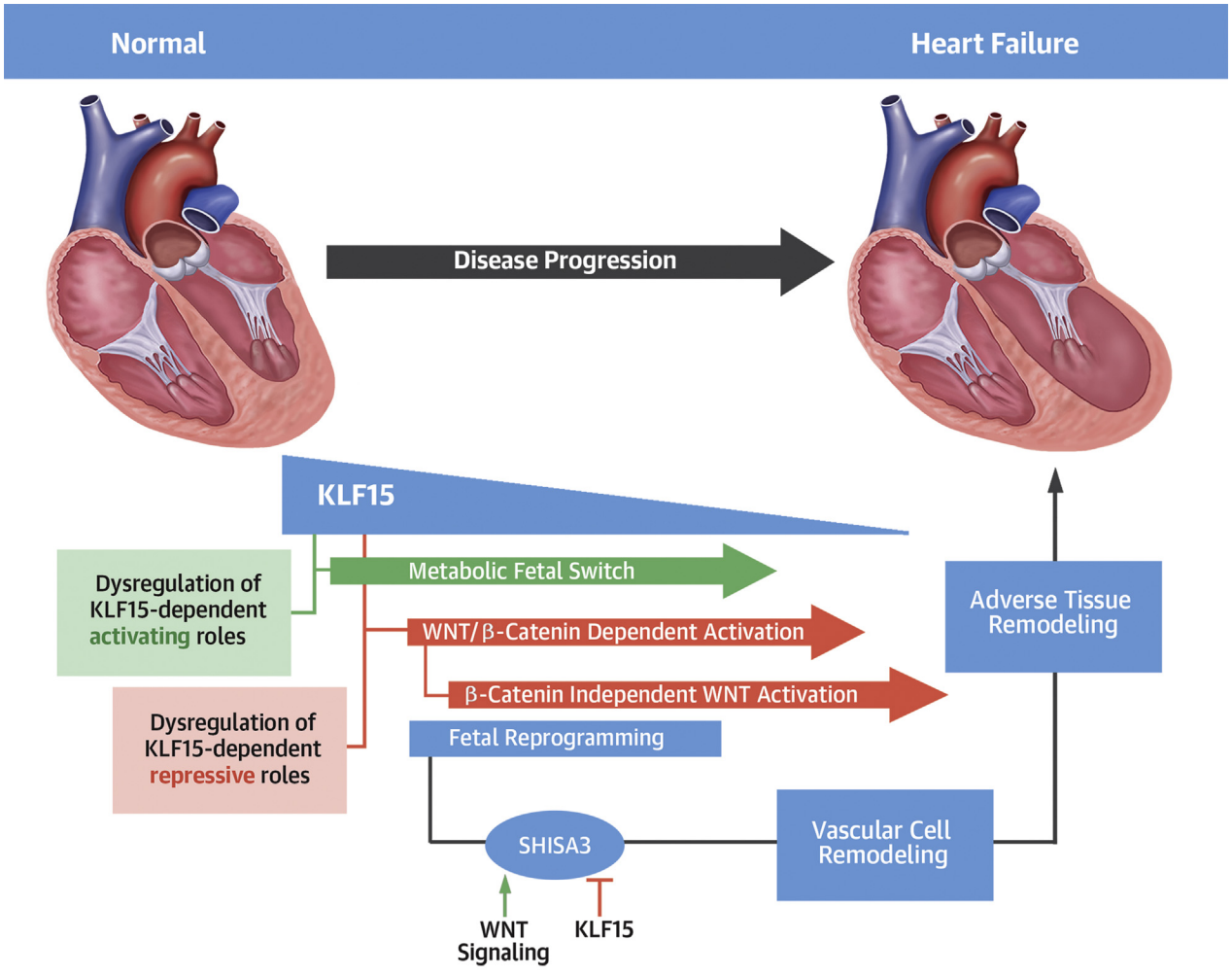

Noack, C. et al. J Am Coll Cardiol. 2019;74(14):1804–19.

Postnatally, KLF15 persistently activates cardiac metabolism, but progressively represses Wnt pathway and pathological, hypertrophic pathways associated with fetal gene reprogramming, which is dysregulated upon pathological remodeling with reduced KLF15 expression. Within this program, we identified a novel early vascular marker, SHISA3, normally expressed in the developing heart and upregulated in pathological remodeling. Overall this reprogramming leads to adverse cardiac remodeling.

identified a novel subpopulation of vascular cells (VCs) marked by SHISA3 expression upon Wnt modulation in CM of *Klf15* KO and β-Cat$^{\Delta ex3}$ mice. Next, non-CM from WT adult hearts were treated with conditioned medium obtained from WT, *Klf15* KO, and β-Cat$^{\Delta ex3}$ cultured CM. *Klf15* KO and β-Cat$^{\Delta ex3}$ CM conditioned medium induced increased *Emcn* transcripts and SHISA3/EMCN coexpressing cells (**Figures 6A and 6B**, Online Figure 7C).

Motif analysis on the promoters of up-regulated DEGs in 4-week and 20-week *Klf15* KO hearts showed enrichment of transcription factors (TFs) regulating muscle and endothelial/hematopoietic development, and chromatin remodeling (i.e., MYOGNF1, GATA1, TAL1) (21–23) (**Figure 6C**). This was accompanied by the up-regulation of the TAL1-cofactor LIM-only-2 protein (*Lmo2*); the bona fide target of the TAL1/LMO2 complexes, angiopoietin-2

(*Angpt2*) (24) and the up-regulation of angiogenic progenitor transcripts *Bambi*, *Edn3*, and *Cd248* (aka *Tem1*), along with increased pS472/pS473-AKT in 20 weeks *Klf15* KO hearts (**Figures 6D to 6F**, Online Figures 5A, 7D, and 7E). A similar program was observed in β-Cat$^{\Delta ex3}$ hearts (Online Figures 7F and 7G). A mouse model with attenuated Wnt activation in CM (β-Cat$^{\Delta ex2\text{-}6}$) that prevents severe HF post-TAC (4) showed reduced levels of *Shisa3* and *Emcn* expression compared with control TAC hearts (**Figure 6G**). Furthermore, mouse fetal E14.5 hearts treated with WNT3A resulted in Wnt/β-catenin activation and *Shisa3* up-regulation compared with controls (**Figures 6H and 6I**). These data strongly support the notion that the loss of KLF15 with consequential activation of Wnt signaling triggers an activation of SHISA3 and VC remodeling.

KLF15-DEPENDENT REPRESSION OF WNT SIGNALING IS RECAPITULATED IN HUMAN CM. Two homozygous KLF15 KO human embryonic stem cell (HES) lines (**Figure 7A**) (25) were used to generate CMs and engineered human myocardium (EHM), which showed significantly impaired functional performance and a blunting of the positive force-frequency relationship compared with WT-EHM (**Figure 7B**, Online Figures 8A to 8C) ($n \geq 6$/group). Transcriptional activation of Wnt/β-catenin signaling as indicated by *AXIN2* up-regulation was also observed in *KLF15*-KO EHM, but not in 2-dimensional embryonic *KLF15*-KO CMs, along with higher TCF7L2 expression in cTnT-positive cells in *KLF15*-KO EHM compared with WT-EHM. This was accompanied by increased, but low, *SHISA3* expression, which can be explained by a small fraction (<5%) of undifferentiated cells that are destined for a different cell fate (**Figures 7C and 7D**).

Transcriptome data showed that HES-derived CMs, which represent an embryonic phenotype, showed low *KLF15* levels, increasing in fetal and adult human ventricular tissue (**Figure 7E**), in line with our observations in mouse at different developmental stages (**Figure 1F**). Importantly, *KLF15* was down-regulated in human hearts of patients with cardiovascular diseases (CVDs) including dilated cardiomyopathy, which is associated with activated Wnt signaling (4). *SHISA3* expression was increased in young, middle-aged, and old patients with CVD (16 to 31, 45 to 65, and 70 to 85 years of age, respectively, $n = 35$) compared with nonfailing hearts ($n = 12$) (**Figures 7F and 7G**, Online Figure 8D). Notably, similar to findings in mice, SHISA3 clearly colocalized with ACTA2^{+} cells in diseased human hearts; the coexpression with PECAM1 was less evident (**Figures 7H and 7I**, Online Figure 8E). Analysis of transcriptomic data showed a relevant expression of *SHISA3* in highly vascularized tissues such as kidney, lung, and heart (Online Figure 8F). These data strongly indicate a *SHISA3* vascular fate and reactivation upon pathological remodeling in the human myocardium.

DISCUSSION

KLF15 and Wnt canonical dysregulation are described in human CVD (11,26–28). However, their mechanistic interplay remained elusive. We described 2 major functions of KLF15 in the postnatal heart: an early and persistent activation of cardiac metabolism, and a later inhibitory role on tissue remodeling, involving Wnt signaling.

In the adult heart, Wnt/β-catenin signaling is low and is reactivated in pathological situations (5). Ectopic cardiac Wnt/β-catenin signaling activation, resulting in increased TCF7L2 expression in CM, induces chromatin and tissue remodeling leading to HF (4,28,29) similar to our observations in *Klf15* KO hearts. This strongly suggests the aberrant contribution of Wnt activation in pathological remodeling of hearts lacking functional KLF15. We demonstrated that KLF15 loss results in Wnt transcriptional activation with impaired function in *KLF15* KO-EHMs, demonstrating a conserved mechanism in human cells.

During embryonic heart development, and also in Wnt-(β-Cat$^{\Delta ex3}$ mice)-activated adult hearts, Wnt/β-catenin-dependent activation is followed by an up-regulation of Wnt/β-catenin-independent signaling and modulators to repress the canonical signaling (4,30). Similarly, Wnt canonical activation is followed by an up-regulation of noncanonical components including WNT5B in *Klf15* KO hearts. This was accompanied by an enrichment of the Rho-A cell polarity pathway and AKT phosphorylation at the time of intense tissue remodeling. These mechanisms are described to regulate cell migration and vessel remodeling (31–33) and may explain the identification of vasculogenesis processes activated by both KLF15 loss and Wnt/β-catenin signaling activation. Our data further verified that cellular crosstalk triggered a vascular program established by *Klf15* KO- and β-Cat$^{\Delta ex3}$-diseased CMs with increased TCF7L2 expression. Prediction of TF binding on DEGs of *Klf15* KO and β-Cat$^{\Delta ex3}$ hearts showed TAL1 and increased expression of *Angpt2*

and *Lmo2*, which participate in VC programming (34). ANGPT2 promotes stable enlargement of normal vessels, but leads to vascular remodeling with leakage in pathological conditions (35). Thus, the transcriptional program activated upon pathological reprogramming under low KLF15 levels and high Wnt activity, may drive a vascular program with insufficient vessel maturation that eventually contributes to HF progression.

This study reveals a novel, evolutionarily conserved VC signature represented by SHISA3 expression, up-regulated in *Klf15* KO and Wnt-activated (β-Cat$^{\Delta ex3}$) hearts as well as in pathologically stressed mouse and human adult hearts. Accordingly, *Shisa3* up-regulation was found in previously published transcriptome data from genetic hypertrophic cardiomyopathies and pressure overload in mice (36,37). SHISA3 cells partially colocalized with the SMC marker ACTA2 in vascular structures and to a lesser extent with EC markers EMCN and PECAM1 in interstitial cells in pathological hearts, whereas SHISA3 and EMCN colocalization was more evident in the developing prenatal heart. EMCN re-expression occurs in the context of MI as part of a neovascularization program (38), suggesting the participation of SHISA3 in neovascularization. SHISA3 itself inhibits Wnt and FGF signaling (39), and was found associated with cancer and human arteriovenous EC identity (40), further indicating a role in vascular-related processes. We showed SHISA3 ectopic activation upon canonical WNT3A stimulation in the fetal heart. Conversely, SHISA3 along with *Emcn* and *Pecam1* expression was reduced upon fetal *Klf15* overexpression, mimicking the adult healthy heart with high KLF15, low Wnt signaling, and lowly expressed SHISA3. Additionally, a clear epigenetic activation of the *Shisa3* gene upon EC differentiation was detected (20). Thus, *Shisa3* re-expression contributes to the recapitulation of developmental vascular mechanisms reactivated in the pathological heart.

The sources of VCs are diverse, whereby SMCs and ECs can share common progenitors. Due to their plasticity, they undergo a phenotypic specialization to meet the needs of specific tissues and conditions, including cell dedifferentiation in cardiovascular pathologies. This can be modulated by Notch, Wnt signaling, and inflammatory cytokines (41,42). Our data suggest that Wnt modulation affects SHISA3 expression in VC lineages in the fetal and adult pathological heart upon vascular remodeling. Further studies are ongoing to establish the origin and function of these cells.

STUDY LIMITATIONS. Because of the potential limitations of a *Klf15* systemic KO model, we used a specific CM-Wnt activated model (β-Cat$^{\Delta ex3}$) as well as in vitro assays using CM fractions for coculturing with VCs. However, we cannot exclude the contribution of other cell types to the activation of the vascular program. Finally, our murine model has a complete lack of KLF15 throughout life, and therefore, an early onset of transcriptional dysregulation and functional deterioration may occur. By contrast, the diseased human heart presented only a reduction on KLF15 expression, and this fact needs to be taken into account for age-matched data comparison.

CONCLUSIONS

Our work revealed a role for KLF15-mediated Wnt/β-catenin-dependent and -independent pathway repression affecting CM dedifferentiation and VC remodeling in the adult heart. In this context, we identified SHISA3 as a novel VC marker of fetal reprogramming in HF in mouse and human hearts (**Central Illustration**). An important finding with therapeutic implications of our study is that the KLF15-mediated Wnt signaling regulation is heart-specific and evolutionarily conserved in human cells. Considering the ubiquitous and broad usage of Wnt signaling in different organs, this serves as an entry point for the identification of heart-specific targeting of Wnt signaling to prevent HF.

ACKNOWLEDGMENTS The authors thank Daniela Liebig-Wolter, Silvia Bierkamp, Daria Reher, and Sandra Georgi for technical assistance, CRC/SFB 1002 Service Units (S01 for echocardiography measurements; S02 for cytoskeleton analysis and INF for platform structure), and Dr. Gabriela Salinas (Next-generation Sequencing Integrative Genomics Core Unit [NIG], University Medical Center Goettingen) for advice on RNA-seq.

ADDRESS FOR CORRESPONDENCE: Dr. Laura C. Zelarayán, Institute of Pharmacology and Toxicology, University Medical Center, Goettingen & DZHK, Robert-Koch-Strasse 40, 37075 Goettingen, Germany. E-mail: laura.zelarayan@med.uni-goettingen.de. Twitter: @LauraZelarayan2.

PERSPECTIVES

COMPETENCY IN MEDICAL KNOWLEDGE: A novel early marker of endothelial cell function, SHISA3, is upregulated in pathological cardiac remodeling, modulated by Wnt and KLF15. This helps elucidate 1 of the mechanisms responsible for neovascularization in cardiac hypertrophy and myocardial remodeling.

TRANSLATIONAL OUTLOOK: Additional experiments are needed to identify the pathways of interaction between KLF15 and SHISA3 during the development of heart failure. This could facilitate development of interventions that promote angiogenic balance and prevent progressive deterioration of function in diseased hearts.

REFERENCES

1. Hirsch E, Nagai R, Thum T. Heterocellular signalling and crosstalk in the heart in ischaemia and heart failure. Cardiovasc Res 2014;102:191–3.

2. Oka T, Akazawa H, Naito AT, Komuro I. Angiogenesis and cardiac hypertrophy: maintenance of cardiac function and causative roles in heart failure. Circ Res 2014;114:565–71.

3. Deb A. Cell-cell interaction in the heart via Wnt/beta-catenin pathway after cardiac injury. Cardiovasc Res 2014;102:214–23.

4. Iyer LM, Nagarajan S, Woelfer M, et al. A context-specific cardiac beta-catenin and GATA4 interaction influences TCF7L2 occupancy and remodels chromatin driving disease progression in the adult heart. Nucleic Acids Res 2018;46:2850–67.

5. Hermans KC, Blankesteijn WM. Wnt signaling in cardiac disease. Compr Physiol 2015;5:1183–209.

6. Noack C, Zafiriou MP, Schaeffer HJ, et al. Krueppel-like factor 15 regulates Wnt/beta-catenin transcription and controls cardiac progenitor cell fate in the postnatal heart. EMBO Mol Med 2012;4:992–1007.

7. Prosdocimo DA, Sabeh MK, Jain MK. Kruppel-like factors in muscle health and disease. Trends Cardiovasc Med 2015;25:278–87.

8. Leenders JJ, Wijnen WJ, Hiller M, et al. Regulation of cardiac gene expression by KLF15, a repressor of myocardin activity. J Biol Chem 2010;285:27449–56.

9. Fisch S, Gray S, Heymans S, et al. Kruppel-like factor 15 is a regulator of cardiomyocyte hypertrophy. Proc Natl Acad Sci U S A 2007;104:7074–9.

10. Wang B, Haldar SM, Lu Y, et al. The Kruppel-like factor KLF15 inhibits connective tissue growth factor (CTGF) expression in cardiac fibroblasts. J Mol Cell Cardiol 2008;45:193–7.

11. Haldar SM, Lu Y, Jeyaraj D, et al. Klf15 deficiency is a molecular link between heart failure and aortic aneurysm formation. Sci Transl Med 2010;2:26ra26.

12. Trapnell C, Pachter L, Salzberg SL. TopHat: discovering splice junctions with RNA-Seq. Bioinformatics 2009;25:1105–11.

13. Bindea G, Mlecnik B, Hackl H, et al. ClueGO: a Cytoscape plug-in to decipher functionally grouped gene ontology and pathway annotation networks. Bioinformatics 2009;25:1091–3.

14. Liberzon A, Birger C, Thorvaldsdottir H, Ghandi M, Mesirov JP, Tamayo P. The Molecular Signatures Database (MSigDB) hallmark gene set collection. Cell Syst 2015;1:417–25.

15. He TC, Sparks AB, Rago C, et al. Identification of c-MYC as a target of the APC pathway. Science 1998;281:1509–12.

16. Zhang L, Prosdocimo DA, Bai X, et al. KLF15 Establishes the Landscape of Diurnal Expression in the Heart. Cell reports 2015;13:2368–75.

17. Creyghton MP, Cheng AW, Welstead GG, et al. Histone H3K27ac separates active from poised enhancers and predicts developmental state. Proc Natl Acad Sci U S A 2010;107:21931–6.

18. Sequeira V, Nijenkamp LL, Regan JA, van der Velden J. The physiological role of cardiac cytoskeleton and its alterations in heart failure. Biochimica et biophysica acta 2014;1838:700–22.

19. Liu C, Shao ZM, Zhang L, et al. Human endomucin is an endothelial marker. Biochemical and biophysical research communications 2001;288:129–36.

20. Kanki Y, Nakaki R, Shimamura T, et al. Dynamically and epigenetically coordinated GATA/ETS/SOX transcription factor expression is indispensable for endothelial cell differentiation. Nucleic acids research 2017;45:4344–58.

21. Fan C, Ouyang P, Timur AA, et al. Novel roles of GATA1 in regulation of angiogenic factor AGGF1 and endothelial cell function. The Journal of biological chemistry 2009;284:23331–43.

22. Ema M, Faloon P, Zhang WJ, et al. Combinatorial effects of Flk1 and Tal1 on vascular and hematopoietic development in the mouse. Genes & development 2003;17:380–93.

23. Min Y, Li J, Qu P, Lin PC. C/EBP-delta positively regulates MDSC expansion and endothelial VEGFR2 expression in tumor development. Oncotarget 2017;8:50582–93.

24. Deleuze V, El-Hajj R, Chalhoub E, et al. Angiopoietin-2 is a direct transcriptional target of TAL1, LYL1 and LMO2 in endothelial cells. PloS one 2012;7:e40484.

25. Noack C, Haupt LP, Zimmermann WH, et al. Generation of a KLF15 homozygous knockout human embryonic stem cell line using paired CRISPR/Cas9n, and human cardiomyocytes derivation. Stem Cell Res 2017;23:127–31.

26. Prosdocimo DA, Anand P, Liao X, et al. Kruppel-like factor 15 is a critical regulator of cardiac lipid metabolism. The Journal of biological chemistry 2014;289:5914–24.

27. Lu Y, Zhang L, Liao X, et al. Kruppel-like factor 15 is critical for vascular inflammation. The Journal of clinical investigation 2013;123:4232–41.

28. Hou N, Ye B, Li X, et al. Transcription Factor 7-like 2 Mediates Canonical Wnt/beta-Catenin Signaling and c-Myc Upregulation in Heart Failure. Circ Heart Fail 2016;9.

29. Jeong MH, Kim HJ, Pyun JH, et al. Cdon deficiency causes cardiac remodeling through hyperactivation of WNT/beta-catenin signaling. Proc Natl Acad Sci U S A 2017;114:E1345–54.

30. Cohen ED, Tian Y, Morrisey EE. Wnt signaling: an essential regulator of cardiovascular differentiation, morphogenesis and progenitor self-renewal. Development 2008;135:789–98.

31. Korn C, Scholz B, Hu J, et al. Endothelial cell-derived non-canonical Wnt ligands control vascular pruning in angiogenesis. Development 2014;141:1757–66.

32. Zhu N, Qin L, Luo Z, et al. Challenging role of Wnt5a and its signaling pathway in cancer metastasis (Review). Experimental and therapeutic medicine 2014;8:3–8.

33. Somanath PR, Razorenova OV, Chen J, Byzova TV. Akt1 in endothelial cell and angiogenesis. Cell cycle 2006;5:512–8.

34. De Val S, Black BL. Transcriptional control of endothelial cell development. Developmental cell 2009;16:180–95.

35. Kim M, Allen B, Korhonen EA, et al. Opposing actions of angiopoietin-2 on Tie2 signaling and FOXO1 activation. The Journal of clinical investigation 2016;126:3511–25.

36. Vakrou S, Fukunaga R, Foster DB, et al. Allele-specific differences in transcriptome, miRNome, and mitochondrial function in two hypertrophic cardiomyopathy mouse models. JCI insight 2018;3.

37. Toischer K, Rokita AG, Unsold B, et al. Differential cardiac remodeling in preload versus afterload. Circulation 2010;122:993–1003.

38. Dube KN, Thomas TM, Munshaw S, et al. Recapitulation of developmental mechanisms to revascularize the ischemic heart. JCI insight 2017;2.

39. Yamamoto A, Nagano T, Takehara S, et al. Shisa promotes head formation through the inhibition of receptor protein maturation for the caudalizing factors, Wnt and FGF. Cell 2005;120:223–35.

40. Aranguren XL, Agirre X, Beerens M, et al. Unraveling a novel transcription factor code determining the human arterial-specific endothelial cell signature. Blood 2013;122:3982–92.

41. Dejana E, Hirschi KK, Simons M. The molecular basis of endothelial cell plasticity. Nature Communications 2017;8:14361.

42. Wang G, Jacquet L, Karamariti E, Xu Q. Origin and differentiation of vascular smooth muscle cells. J Physiol 2015;593:3013–30.

KEY WORDS fetal gene reprogramming, heart failure, hypertrophic heart remodeling, vascular cells, Wnt signaling

APPENDIX For an expanded Methods section as well as supplemental figures and tables, please see the online version of this paper.